Protein Composition of Circulating Extracellular Vesicles Immediately Changed by Particular Short Time of High-Intensity Interval Training Exercise

Yoshinao Kobayashi[1,2], Akiko Eguchi[2,3]*, Yasuyuki Tamai[2], Sanae Fukuda[4], Mina Tempaku[2], Kiyora Izuoka[2], Motoh Iwasa[2], Yoshiyuki Takei[2] and Kenji Togashi[5]

[1] Center for Physical and Mental Health, Mie University Graduate School of Medicine, Tsu, Japan, [2] Department of Gastroenterology and Hepatology, Mie University Graduate School of Medicine, Tsu, Japan, [3] JST, PRETO, Kawaguchi, Japan, [4] Department of Health Welfare Sciences, Kansai University of Welfare Sciences, Kashiwara, Japan, [5] Department of Health and Physical Education, Mie University Faculty of Education, Tsu, Japan

Introduction/Purpose: High-intensity interval training (HIIT) promotes various biological processes and metabolic effects in multiple organs, but the role of extracellular vesicles (EVs) released from a variety of cells is not fully understood during HIIT exercise (HIIT-Ex). We investigated the changes in circulating number and proteomic profile of EVs to assess the effect of HIIT-Ex.

Methods: Seventeen young men (median age, 20 years) were enrolled in the study. Total duration of the HIIT-Ex was 4 min. Blood samples were collected from before HIIT-Ex (pre-HIIT-Ex), at the immediate conclusion of HIIT-Ex (T_0), at 30 min (T_{30}), and at 120 min after HIIT-Ex. The pulse rate and systolic blood pressure were measured. Circulating EVs were characterized, and EV proteins were detected *via* nano liquid chromatography tandem mass spectrometry.

Results: The pulse rate and systolic blood pressure at T_0 to pre-HIIT-Ex were significantly higher. Circulating EV number was significantly altered throughout the HIIT-Ex, and the source of circulating EVs included skeletal muscle, hepatocytes, and adipose tissue. Proteomic analysis identified a total of 558 proteins within isolated circulating EVs from pre-HIIT-Ex, T_0, and T_{30}. Twenty proteins in total were significantly changed at pre-HIIT-Ex, T_0, and T_{30} and are involved in a variety of pathways, such as activation of coagulation cascades, cellular oxidant detoxification, and correction of acid–base imbalance. Catalase and peroxiredoxin II were increased at T_0.

Conclusion: The circulating EV composition can be immediately changed by particularly a short time of HIIT-Ex, indicating that EVs may intercommunicate across various organs rapidly in response to HIIT-Ex.

Keywords: extracellular vesicle, proteomic analyses, antioxidant, short time of high intensity interval training exercise, skeletal muscle

INTRODUCTION

High-intensity interval training (HIIT) comprises repeated bouts of high-intensity exercise (e.g., running, cycling, or swimming) and recovery periods of either lower-intensity exercise or rest, which can be carried out using a variety of protocols that manipulate the duration of sprint and recovering interval, the intensity of exercise, and the number of repeated sets (Buchheit and Laursen, 2013a). HIIT promotes the processes of oxygen transport and utilization, which improves overall physical fitness by elevating maximal oxygen consumption (VO_{2max}) (Laursen and Jenkins, 2002). HIIT is known to improve the metabolic function of multiple organs including the heart, lungs, and skeletal muscle (Buchheit and Laursen, 2013a,b). HIIT, combined with caloric restriction, leads to increased glucose and lipid storage in skeletal muscle, as well as elevated adipose thermogenesis (Davis et al., 2017). HIIT has also been shown to improve insulin sensitivity among the elderly (Sogaard et al., 2018), indicating that HIIT promotes various alterations in biological processes and overall metabolism within multiple organs.

Extracellular vesicles (EVs) including exosomes as endosomal origins and microvesicles as blebbing from plasma membrane, which have been shown to be released from a variety of cells, are composed of a lipid bilayer embedded with membrane proteins and an aqueous core containing water-soluble proteins and nucleic acids (Tkach and Thery, 2016; Kalluri and LeBleu, 2020). EVs circulate within the blood; therefore, circulating EVs are useful as non-invasive biomarkers given their specific protein and nucleic acid composition. EVs indicate myriad pathological conditions from the presence of subclinical metabolic risk to the progression of an underlying disease and can predict the EV source: organs/tissues/cells (Kalluri and LeBleu, 2020). EVs are also a tool for cell-to-cell communication through the transfer of various proteins and genes, such as microRNAs and mitochondrial DNAs, to recipient cells that can then regulate a wide assortment of cellular processes (Kalluri and LeBleu, 2020). In general, EVs released from damaged/activated cells contribute to disease progression, while EVs released from embryonic and mesenchymal stem cells repair cellular damage and tissue injury (Kalluri and LeBleu, 2020). We have reported that circulating EV number was significantly associated with various metabolic parameters, including obesity and lipid and glucose metabolism in humans under healthy and aberrant metabolic conditions (Kobayashi et al., 2018). In addition, we found that circulating EV number was significantly associated with skeletal muscle volume, but only in healthy individuals, suggesting that skeletal muscle

releases EVs to maintain normal physical response (Kobayashi et al., 2018). Indeed, exercise stimulates EV release from a variety of tissues including skeletal muscle and also changes EV composition (Fruhbeis et al., 2015; Whitham et al., 2018; Vechetti, 2019; Denham and Spencer, 2020). In addition, skeletal muscle releases various types of EVs (Rome et al., 2019), and C2C12 myoblast and myotube release exosome-like vesicles (Forterre et al., 2014) and microvesicles (Guescini et al., 2010; Highton et al., 2019), but the investigations into the impact of EVs on skeletal muscle are still insufficient, with only a handful of studies that investigated encapsulated microRNAs and a short list of proteins (Vechetti et al., 2020).

There have been several studies concerning EV release in human exercise models (Nederveen et al., 2020) such as 2-km run (Whitham et al., 2018) or 1 h bout of cycling Ex (Wu and Liu, 2018), although the profile of EVs is not fully identified during HIIT exercise (HIIT-Ex). In addition, prompt change of circulating EVs after HIIT-Ex with 4-min duration has not been examined.

In this study, we investigate the association between circulating EVs and a multiorgan response, including lipid and glucose metabolism during HIIT exercise (HIIT-Ex). We also provide data on the prompt change in circulating EV numbers and EV protein composition after HIIT-Ex with short duration.

MATERIALS AND METHODS

Study Participants

Seventeen young male individuals (median age, 20 years) enrolled in the study. They were students of Mie University (Mie, Japan) majoring in health and physical education. They were physically active and were trained as players of the Mie University baseball team. The basic characteristics of the study participants are shown in **Table 1**. The study was approved by the Ethics Committee at Mie University (approval no. 3201). All study participants provided written informed consent prior to enrollment. All methods were performed in accordance with the relevant guidelines and regulations.

HIIT-Ex Protocol and Blood Collection

Exercise was undertaken on a programmable bicycle ergometer (Powermax VII, Konami Corporation, Tokyo, Japan). Prior to the HIIT-Ex, VO_{2max} value for each participant was obtained by gas exchange analysis during bicycle ergometer tests. A number of protocols exist for estimating VO_{2max}. In the present study, initial power output was set at 30 W, and the output was then gradually increased by 2 W every 4 s afterward up to all-out max effort. The pedal cycling speed was fixed at 60 revolutions per minute (rpm) throughout the analysis.

The protocol of HIIT-Ex is shown in **Figure 1**. The protocol in the present study was modified from a protocol described by Tabata et al. (1996). Briefly, the warm-up was done by cycling at a rate of 60 rpm for 10 min. The power output during the warm-up was set at 100 W. After a 5-min rest, a single session of HIIT-Ex was done. Eight sets composed of an exercise bout (cycling at 140% of VO_{2max} for 20 s) and rest for 10 s were performed during

TABLE 1 | Basic characteristics of subjects.

Parameter	Unit	Values (min–max)
N		17
Age	(y)	20 (20–21)
BMI	(kg/m^2)	22.0 (19.6–26.6)
Lean body mass	(kg/m^2)	19.4 (17.5–20.4)
SMV	(kg/m^2)	18.4 (16.6–19.4)
Fat mass	(%)	14.4 (6.3–22.1)
Pulse rate	(beats/min)	72 (55–107)
Systolic BP	(mmHg)	123 (98–143)
Diastolic BP	(mmHg)	63 (50–80)
AST	(IU/L)	21 (13–25)
ALT	(IU/L)	16 (11–31)
g-GPT	(IU/L)	19 (12–44)
LDL-Chol	(mg/dl)	94 (42–135)
TG	(mg/dl)	67 (37–191)
Cr	(mg/dl)	0.85 (0.80–1.12)
FBG	(mg/dl)	83 (65–93)
Fasting IRI	(mU/ml)	4.09 (1.47–12.70)
HOMA-IR		0.84 (0.29–2.60)
HOMA-b		78.8 (31.1–394.2)

the HIIT session. Serum was separated from whole blood and was immediately frozen at −80°C until analysis.

Collecting Anthropometric and Laboratory Data

We measured anthropometric data including body mass index (BMI), lean body mass, skeletal muscle volume (SMV), fat mass, pulse rate, systolic blood pressure (BP), and diastolic BP. Lean body mass, SMV, and fat mass were measured using multiple-frequency bioimpedance technology (MC-190 body composition analyzer, TANITA Corporation, Tokyo, Japan). Measurements of pulse rate, systolic BP, and diastolic BP, as well as blood collection were performed before HIIT-Ex (pre-HIIT-Ex), at the

immediate conclusion of HIIT-Ex (T_0), at 30 min (T_{30}), and at 120 min (T_{120}) after HIIT-Ex. Serum was separated from blood and immediately stored at −80°C for analysis.
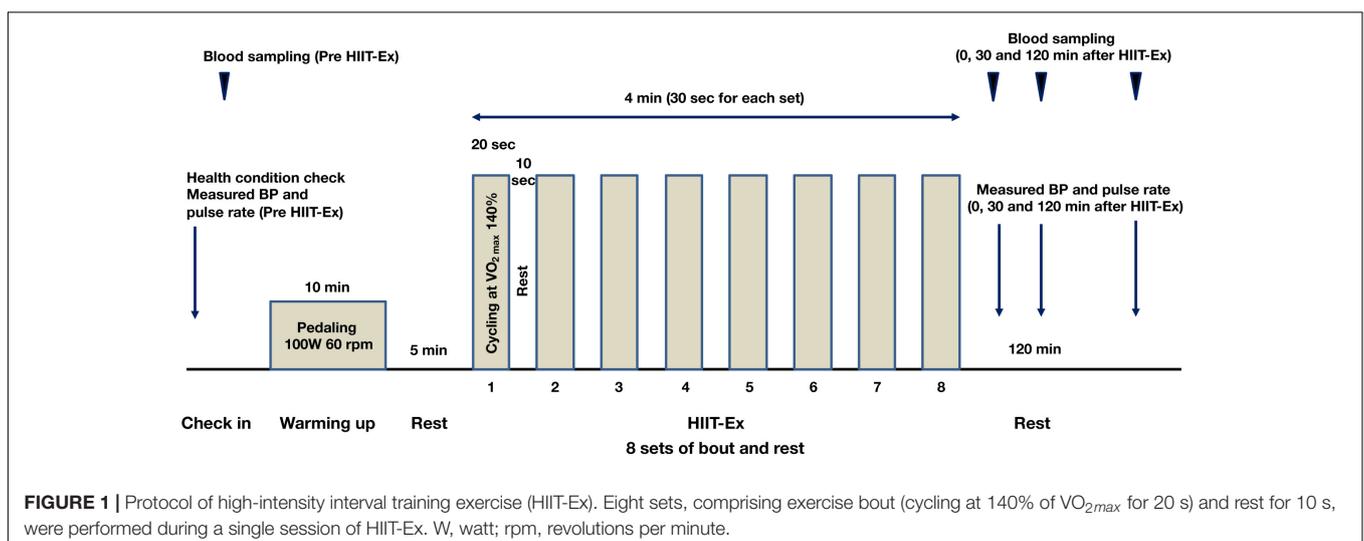
Serum levels of aspartate aminotransferase (AST), alanine aminotransferase (ALT), γ-glutamyl transpeptidase (γ-GTP), low-density lipoprotein cholesterol (LDL-Chol), triglyceride (TG), creatinine (Cr), fasting blood glucose (FBG), free fatty acid (FFA), creatine phosphokinase (CPK), and fasting immunoreactive insulin (IRI) were measured at SRL Inc. (Tokyo, Japan). The homeostatic model assessment of insulin resistance (HOMA-IR) was calculated as [fasting IRI (μU/ml) × FBG (mg/dl)]/405 (Matthews et al., 1985). The homeostasis model assessment–β-cell function (HOMA-β) was calculated as [fasting IRI (μU/ml) × 360/FBG (mg/dl)] – 63 (Matthews et al., 1985).

Flow Cytometry Analysis of Circulating EVs

Serum was centrifuged at 2,000 × g for 10 min to eliminate any aggregations. Circulating EVs in 2 μl of serum were stained with 4 μg/ml of calcein-AM (Invitrogen, San Diego, CA, United States) for 30 min in the dark at room temperature. The number of EVs was determined by flow cytometry (BD Cant II; BD Biosciences, San Jose, CA, United States) with flow cytometry alignment beads (Thermo Fisher Scientific, Tokyo, Japan) by triplication in each sample, and data were analyzed using FlowJo software (TreeStar, Ashland, OR, United States).

Isolation of Circulating EVs and Measurement of Size

Serum was centrifuged at 2,000 × g for 10 min to eliminate any aggregations. Circulating EVs were isolated from an equal amount (500 μl) of serum between samples *via* qEV columns (Izon Science, Christchurch, New Zealand) according to the manufacturer's instruction. All fractions, fractions 1–30, were collected with 500 μl each, and protein amount was measured at OD_{280} according to the manufacturer's instruction. Fractions 6–10 were concentrated with Amicon Ultracel-3K (EMD

FIGURE 1 | Protocol of high-intensity interval training exercise (HIIT-Ex). Eight sets, comprising exercise bout (cycling at 140% of VO$_{2max}$ for 20 s) and rest for 10 s, were performed during a single session of HIIT-Ex. W, watt; rpm, revolutions per minute.

Millipore, Temecula, CA, United States). The diameter of isolated circulating EVs was measured *via* nanoparticle tracking analysis, Nanosight LA10 (Malvern Panalytical, Malvern, United Kingdom) by triplication in each sample.

Analysis of Protein Composition in Circulating EVs *via* Nano Liquid Chromatography Tandem Mass Spectrometry (Nano-LC-MS/MS)

The method for isolating EVs from serum was described above. We randomly picked up 3 subjects from the 11 subjects with elevated circulating EV numbers at T_0 compared to pre-HIIT-Ex. Briefly, circulating EVs were isolated from an equal amount (500 μl) of plasma between samples *via* qEV columns (Izon Science) according to the manufacturer's instruction. Fractions 6–10 were collected from the columns, and EVs were precipitated using trichloroacetic acid, followed by reduction, alkylation with iodoacetamide, and trypsinization using an equal amount of protein between samples. Samples were separated using nano-LC-MS/MS, EASY-nLC 1200 (Thermo Fisher Scientific), and Q Exactive Plus (Thermo Fisher Scientific) at APRO Science Institute (Tokushima, Japan). Data were analyzed using Scaffold4 (Proteome Software, Portland, OR, United States) against the SwissProt database at APRO Science Institute. Quantitative value (normalized total spectra) on Scaffold4 (Proteome software Inc., Portland, OR, United States) was used for heatmap and protein interactions, which were generated using Heatmapper software (Babicki et al., 2016) and STRING v11.0 software (Szklarczyk et al., 2019), respectively.

Western Blotting Analysis of Isolated EVs

Isolated EVs (10.4 μg) were lysed with radioimmunoprecipitation assay (RIPA) lysis buffer resolved in TGX^{TM} precast gels and transferred to polyvinylidene difluoride membrane (BioRad, Hercules, CA, United States). Blotted membranes were incubated with blocking reagent for Can Get signal (TOYOBO, Osaka, Japan) and primary antibodies followed by peroxidase-conjugated secondary antibody (GE Healthcare Life Sciences, Pittsburgh, PA, United States) in Can Get solutions. The primary antibodies used were anti-CD9 (BioLegend, San Diego, CA, United States; 312102, ×500), anti-CD81 (SBI, Palo Alto, CA, United States; EXOAB-CD81A-1, ×1,000), anti-TSG101 (SBI; EXOAB-TSG101-1, ×1,000), anti-syntenin-1 (Santa Cruz, Dallas, TX, United States; 515538, ×1,000), anti-asialoglycoprotein receptor 1 (ASGPR1) (Genetex, Irvine, CA, United States; 122674, ×1,000), anti-perilipin (Abcam; 61682, ×1,000), anti-α-skeletal muscle actin (Abcam; 52218, × 500), anti-peroxiredoxin II (PRDX-2) (Santa Cruz; 515428, ×1,000), and anti-catalase (CAT) (Santa Cruz; 271803, ×1,000). The membrane was treated with Stripping buffer (Nakalai Tesque, Kyoto, Japan) or azide-TBST to remove horseradish peroxidase (HRP). Protein bands were visualized using enhanced chemiluminescence reagents (Thermo Fisher Scientific, Waltham, MA, United States) and digitized using a charge-coupled device camera (LAS4000 mini; Fuji Film, Tokyo,

Japan). Expression intensity was quantified by Multi Gauge software (Fuji).

Statistical Analysis

Data are expressed as medians with ranges. Parameter values determined at pre-HIIT-Ex, T_0, T_{30}, and T_{120} were compared using Kruskal–Wallis test. For proteomic data, parameter values in the entire three time points (at pre-HIIT-Ex, T_0, and T_{30}) were tested *via* mixed model repeated-measure analysis to determine the effect of time. Values with $p < 0.05$ were considered statistically significant. Statistical analysis was done using Multivariable Analysis for Mac version 3.0 software (Esumi, Tokyo, Japan) and SPSS version 22.0 J software (SPSS Japan, Tokyo, Japan).
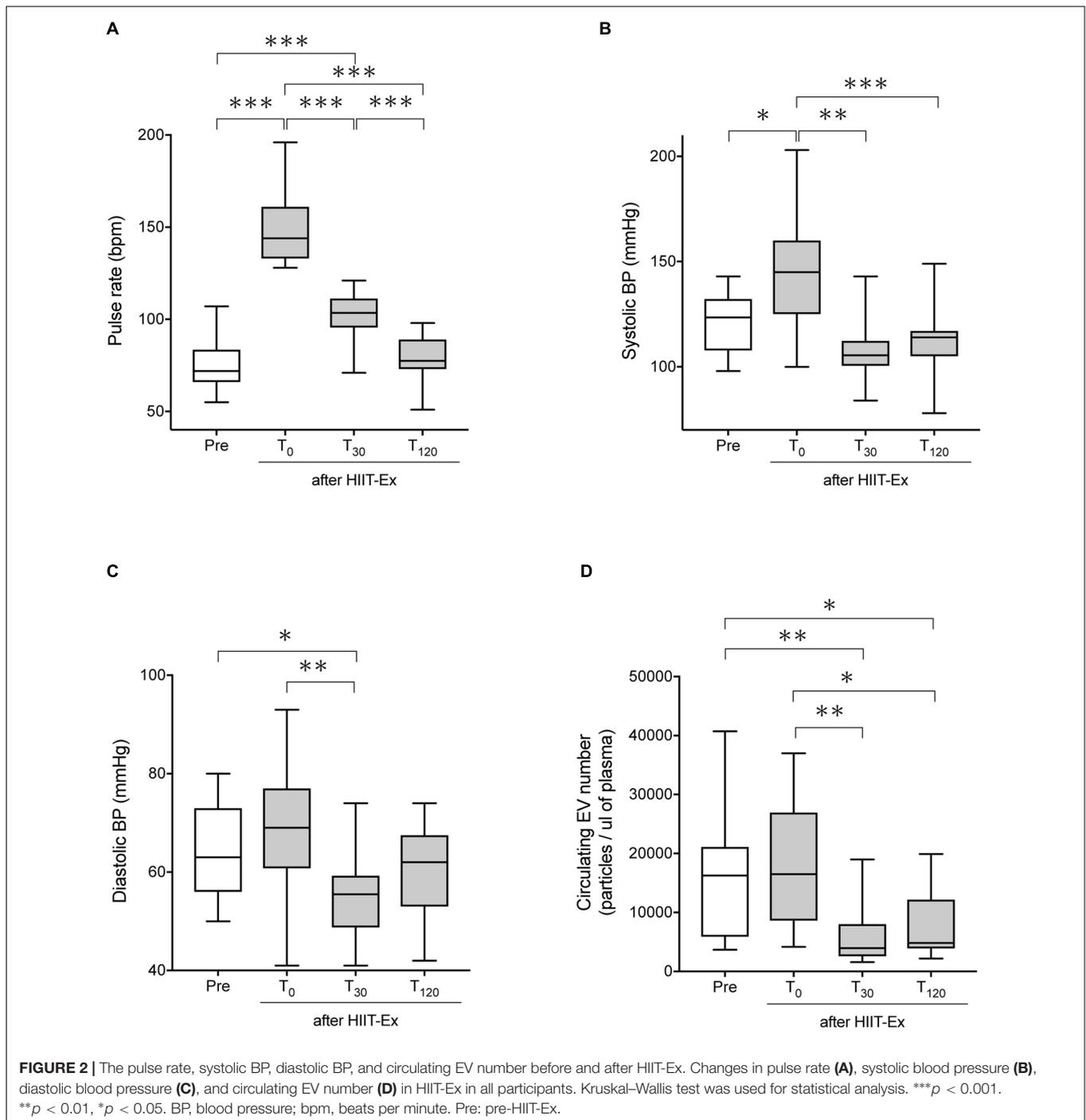
RESULTS

Basic Characteristics of All Participants

The basic characteristics of all subjects are summarized in **Table 1**. Values of liver enzymes, LDL-Chol, Cr, and FBG were within the normal range for all subjects. Two subjects had metabolic factor(s): one individual showed overweight (25.0 ≦ BMI < 30.0 kg/m^2) (No authors listed, 2000), elevated serum TG ≧ 150 mg/dl, and elevated HOMA-R ≧ 2.5 (Matthews et al., 1985), and another individual showed elevated serum TG ≧ 150 mg/dl.

Pulse Rate, Blood Pressure, Serum FFA Levels, and Circulating EV Number Were Changed by HIIT-Ex

The protocol of HIIT-Ex is shown in **Figure 1**. Pulse rate and systolic BP were significantly elevated at T_0 when compared to the values at pre-HIIT-Ex (pulse rate: $p < 0.001$, systolic BP: $p < 0.05$) (**Figures 2A,B**). Diastolic BP was not significantly increased at T_0, whereas reduced at T_{30} ($p < 0.05$) when compared to the values at pre-HIIT-Ex (**Figure 2C**). Median values of systolic BP at T_{30} and T_{120} were lower than pre-HIIT-Ex, although the differences were not significant (**Figure 2B**). Serum levels of all other biochemical parameters including AST, CPK, Cr, LDL-Chol, and TG were not significantly changed after HIIT-Ex. Notably, serum FFA levels at T_{120} were significantly elevated compared to levels pre ($p < 0.05$), at T_0 ($p < 0.01$), and at T_{30} ($p < 0.01$) (**Supplementary Table 1**). Next, we investigated the changes in circulating EV number as a result of HIIT-Ex using calcein AM, which was non-fluorescent until it passively enters EVs, after which it is activated by esterase and becomes fluorescent and EV impermeant (Gray et al., 2015; **Figure 2D**). The median value for circulating EV number in all subjects at pre-HIIT-Ex was 16,253 particles/μl, with a range of 3,654–40,725 particles/μl. EV number was significantly reduced at T_{30} and T_{120} when compared to pre-HIIT-Ex ($p < 0.01$: T_{30} vs. pre-HIIT-Ex, $p < 0.05$: T_{120} vs. pre-HIIT-Ex). EV numbers at T_0 was not significantly different from the values at pre-HIIT-Ex, although we found that circulating EV number was
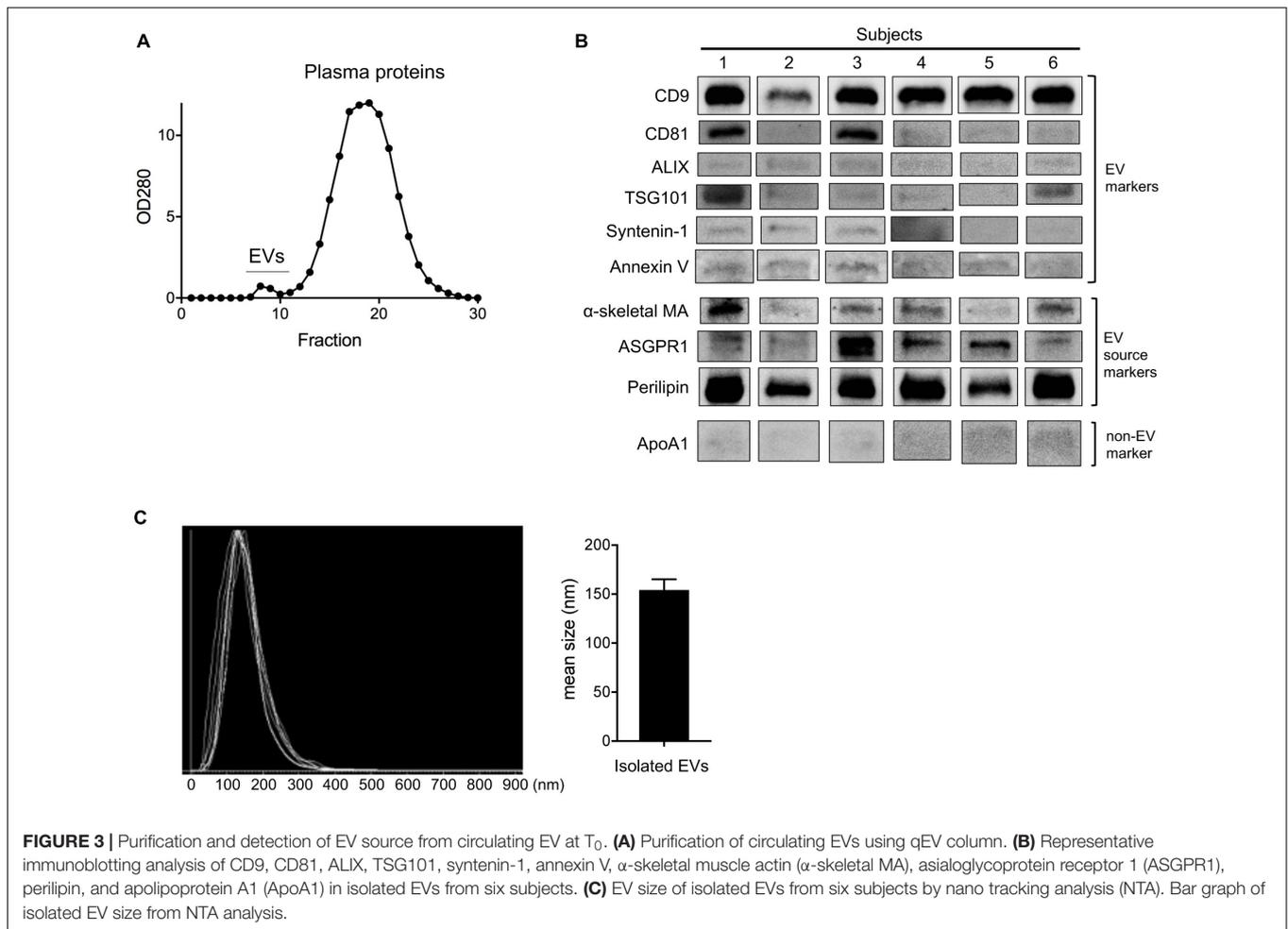
FIGURE 2 | The pulse rate, systolic BP, diastolic BP, and circulating EV number before and after HIIT-Ex. Changes in pulse rate **(A)**, systolic blood pressure **(B)**, diastolic blood pressure **(C)**, and circulating EV number **(D)** in HIIT-Ex in all participants. Kruskal–Wallis test was used for statistical analysis. ***$p < 0.001$. **$p < 0.01$, *$p < 0.05$. BP, blood pressure; bpm, beats per minute. Pre: pre-HIIT-Ex.

promptly increased in 11 out of 17 (64.7%) subjects at T_0 when compared to pre-HIIT-Ex.

Circulating EVs Were Derived From Skeletal Muscle, Hepatocytes, and Adipose Tissue

Changes in circulating EV number as a result of HIIT-Ex led us to further investigate the tissue and/or cellular source of EV

release, as well as the overall EV protein composition. Therefore, we isolated circulating EVs from serum using qEV columns (**Figure 3A**) and detected exercise-induced metabolic proteins related to skeletal muscle, adipose, and liver in representative six subjects. We detected CD9, CD81, ALIX, TSG101, syntenin-1, annexin V (EV markers), α-skeletal muscle actin (α-skeletal MA—enriched in skeletal muscle) (Ilkovski et al., 2005), ASGPR1 (enriched in hepatocytes) (Ashwell and Morell, 1974; Povero et al., 2014), and perilipin A (enriched mainly in the adipose

FIGURE 3 | Purification and detection of EV source from circulating EV at T_0. **(A)** Purification of circulating EVs using qEV column. **(B)** Representative immunoblotting analysis of CD9, CD81, ALIX, TSG101, syntenin-1, annexin V, α-skeletal muscle actin (α-skeletal MA), asialoglycoprotein receptor 1 (ASGPR1), perilipin, and apolipoprotein A1 (ApoA1) in isolated EVs from six subjects. **(C)** EV size of isolated EVs from six subjects by nano tracking analysis (NTA). Bar graph of isolated EV size from NTA analysis.

tissue) (Kimmel et al., 2010; Eguchi et al., 2016) in circulating EVs taken at T_0 (**Figure 3B** and **Supplementary Figure 1**), suggesting that a part of circulating EVs were derived from multiple tissues and cells including the skeletal muscle, hepatocytes, and adipose tissue as a function of HIIT-Ex. Although we used qEV column that has less lipoprotein overlap for EV isolation, a small amount of apolipoprotein A1 was still detected as a contamination in all circulating EVs (**Figure 3B** and **Supplementary Figure 1**). The diameters of circulating EVs from six subjects were similar with average mean of 154.2 nm (**Figure 3C**).

HIIT-Ex Induced Changes in Circulating EV Protein Composition Involving Cellular Oxidant Detoxification, Regulation of Exocytosis, Regulation of Stress, Regulation of Vesicle-Mediated Transport, Extracellular Matrix Organization, and Response to Stimulus

Next, we explored circulating EV composition in three individuals using proteomic analysis. Three individuals were randomly picked from the 11 participants with elevated

circulating EV numbers at T_0 compared to pre-HIIT-Ex. The circulating EVs from each participant were elevated at T_0 when compared to pre-HIIT-Ex and were decreased at T_{30} (**Figure 4A**). These results were ascertained in terms of the EV proteome by nano-LC-MS/MS analysis. The proteomic analysis identified a total of 558 proteins contained within isolated circulating EVs from pre-HIIT-Ex, T_0, and T_{30}. Of the 558 proteins, a total of 361 proteins were found to be common among circulating EVs taken from all time points. Drilling down further within this protein pool, we determined a total of 34, 28, and 65 proteins unique to pre-HIIT-Ex, T_0, and T_{30}, respectively (**Figure 4B**). We observed significant changes in a total of 20 proteins including alpha-2-antiplasmin, von Willebrand factor (VWF), multimerin-1 (MMR1), fibrinogen alpha chain (FGA), fibrinogen beta chain (FGB), fibrinogen gamma chain (FGG), carbonic anhydrase-1 (CA-1), PRDX-2, catalase (CAT) the above-mentioned CAT, and CA-1 within circulating EVs among samples taken at pre-HIIT-Ex, T_0, and T_{30} (**Figure 4C**). FGG, an essential component to form an insoluble fibrin matrix in hemostasis, was increased significantly at T_0 compared to pre-HIIT-Ex ($p < 0.01$) (**Figure 4D**). An antioxidative protein CAT was gradually increased to be significantly elevated at T_{30} compared to pre-HIIT-Ex ($p < 0.05$) (**Figure 4D**). CA-1, as
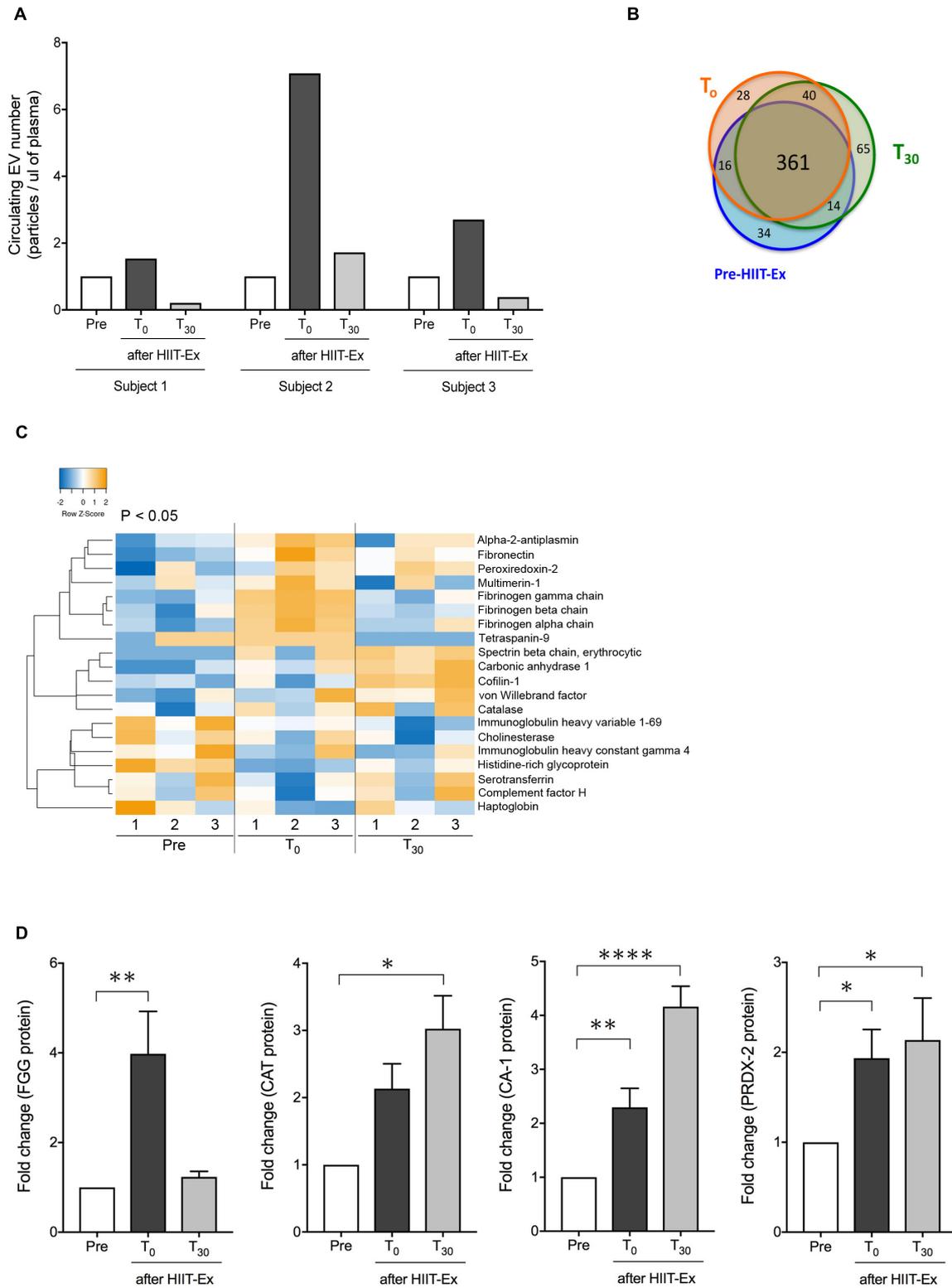
FIGURE 4 | Detected EV proteins. **(A)** Changes in circulating EV number at pre-HIIT-Ex, T_0, and T_{30} in three subjects using proteomic analysis. **(B)** Detected protein number at pre-HIIT-EX, T_0, and T_{30}. **(C)** Heatmap of identified proteins with significant changes in isolated circulating EVs at pre-HIIT-Ex, T_0, and T_{30}. **(D)** Change in EV protein values at pre-HIIT-Ex, T_0, and T_{30}. Fibrinogen gamma chain (FGG), catalase (CAT), carbonic anhydrase (CA-1), and peroxiredoxin II (PRDX-II). Kruskal-Wallis test was used for evaluating statistical significance among the three sampling points. ****$p < 0.0001$, **$p < 0.01$, *$p < 0.05$. Pre: pre-HIIT-Ex.

Protein ID	p-value (Pre. vs. T_0)
Alpha-2-antiplasmin	0.011*
Fibronectin	0.011*
Peroxiredoxin-2	0.021*
Fibrinogen gamma chain	0.009**
Fibrinogen beta chain	0.029*
Fibrinogen alpha chain	0.021*
Carbonic anhydrase 1	0.004**
Immunoglobulin heavy constant gamma 4	0.021*
Histidine-rich glycoprotein	0.003**
Serotransferrin	0.019*
Haptoglobin	0.018*
Reelin	0.049*

*$p < 0.05$, **$p < 0.01$, analyzed by Kruskal–Wallis test.

an essential protein for maintaining acid–base homeostasis, was significantly increased both at T_0 and T_{30} compared to pre-HIIT-Ex ($p < 0.01$ T_0 vs. Pre-HIIT-Ex, $p < 0.0001$ T_{30} vs. pre-HIIT-Ex) (**Figure 4D**). An antioxidant protein PRDX-2 was significantly increased both at T_0 and T_{30} compared to pre-HIIT-Ex ($p < 0.05$ T_0 vs. pre-HIIT-Ex, $p < 0.05$ T_{30} vs. pre-HIIT-Ex) (**Figure 4D**). We listed 12 proteins that were significantly increased at the immediate conclusion of HIIT-Ex (T_0) (each $p < 0.05$) (**Table 2**).

From the protein–protein interaction analysis using STRINGS, the 20 proteins, which were significantly changed during HIIT-Ex, elucidated various protein–protein interaction clusters including cellular oxidant detoxification, regulation of exocytosis, regulation of stress, regulation of vesicle-mediated transport, extracellular matrix organization, and response to stimulus (**Figure 5A** and **Supplementary Table 2**). Notably, we found that antioxidant enzymes, CAT and PRDX-2, were increased at T_0 and T_{30} (**Figure 4D**), leading us to further validate the abundance of CAT and PRDX-2 in circulating EVs using Western blotting. We detected abundance of CAT and PRDX-2 at pre-HIIT-Ex and T_0 in representative four subjects (**Figure 5B** and **Supplementary Figure 2**). The abundance ratio of antioxidant proteins CAT and PRDX-2 in the isolated circulating EVs of all subjects was increased at T_0 (**Figure 5C**).

DISCUSSION

In the current study, we investigated the changes in circulating number and proteomic profile of EVs to assess the effect of HIIT-Ex. We have demonstrated that the circulating EV number is significantly changed at 30 or 120 min after HIIT-Ex, and overall EV protein composition including FGG, CAT, CA-1, and PRDX-2 is significantly increased at 0 or 30 min after HIIT-Ex. We also showed that a part of circulating EVs were derived from multiple organs including skeletal muscle, adipose tissue, and the liver, suggesting possible interorgan network by HIIT-Ex. We have previously reported a strong correlation between the level of circulating EVs and lipid metabolism, especially with respect to serum TG levels (Kobayashi et al., 2018). Indeed, in the present

study, circulating EV number was reduced at T_{30} in concordance with the reduction in serum levels of TG and FFA. Notably, serum FFA levels were significantly increased at T_{120}, suggesting that HIIT-Ex can facilitate FFA release from the organs, including white adipose tissue, to compensate for overall energy loss as a result of HIIT-Ex.

The number of circulating EVs was elevated just after HIIT-Ex in 11 out of 17 subjects (64.7%). It was surprising that EVs were promptly released into the systemic circulatory pathway in response to only 4 min of exercise intervention. Although we did not observe significant elevation of circulating EV number in all subjects, this result would be expected because HIIT-Ex was performed only for 4 min and circulating EV number at pre-HIIT-Ex was influenced by healthier condition, such as TG levels and inflammation. Furthermore, the efficacy of cardiopulmonary and skeletal muscle loads was different in each subject. Circulating EV number was significantly reduced at T_{30} in all subjects, suggesting that EVs can be received and processed by their target cells, or simply degraded.

Notably, EV proteins were dramatically changed by HIIT-Ex. EV contains a variety of protein types involved in platelet aggregation and coagulation cascades (MMRN1, VWF, FGA, FGB, FGG, and alpha-2-antiplasmin), acid–base homeostasis (CA-1), and antioxidant (CAT and PRDX-2). FGG, which is involved in coagulation cascades including fibrinolysis, was elevated at T_0. HIIT-Ex is known to promote changes in hemostatic and fibrinolytic properties. Short-duration HIIT-Ex significantly increased plasma concentrations of tissue factor, tissue factor pathway inhibitor, thrombin–anti-thrombin complex, and D-dimer (Zadow et al., 2018), resulting in the changes in hemostatic and fibrinolytic properties. The significant increase in EV proteins involved in coagulation cascades found in the present study suggests the activation of the coagulation pathway just after HIIT-Ex, which is in line with previous studies. CA-1 in EVs was also increased after HIIT-Ex. CA-1, one of the cytosolic carbonic anhydrase isozymes, catalyzes the interconversion between $[CO_2 + H_2O]$ and $[H^+ + HCO_3^-]$, which is an essential reaction for maintaining acid–base homeostasis in multiple organs. Intensive muscular exercise induces the formation of lactate and CO_2, which leads to intracellular acidosis. A previous study reported increased blood CA activity 2 weeks after starting interval training (Tas et al., 2019). Therefore, the prompt elevation of CA-1 in EVs may be an adaptive reaction to correct for an acid–base imbalance brought on by HIIT-Ex.

Muscular Ex is associated with an increase in overall oxidative stress (Dillard et al., 1978). Intracellular radicals comprise reactive oxygen species and reactive nitrogen species. Many studies have demonstrated that short-duration and high-intensity Ex promoted an increase in oxidative stress in both blood and skeletal muscle (Powers et al., 2016) due to the contraction of skeletal muscle producing free radicals (Reid et al., 1992). Intracellular radicals play an adverse role in regulating muscle fatigue and the production of skeletal muscle force (Powers and Jackson, 2008). Therefore, antioxidant mechanisms are required to ameliorate muscle cell damage. Human CAT predominantly catalyzes the dismutation of hydrogen peroxide
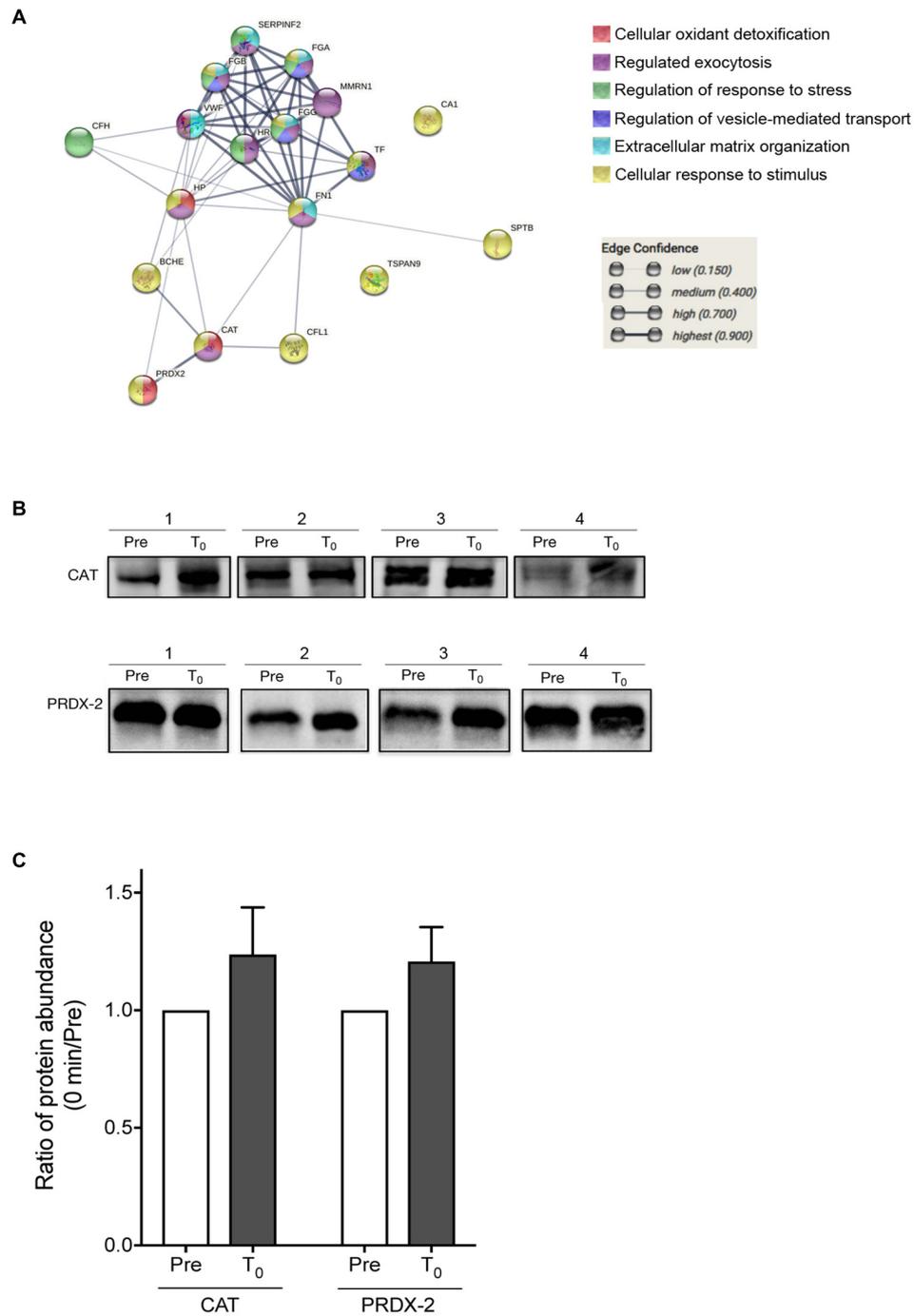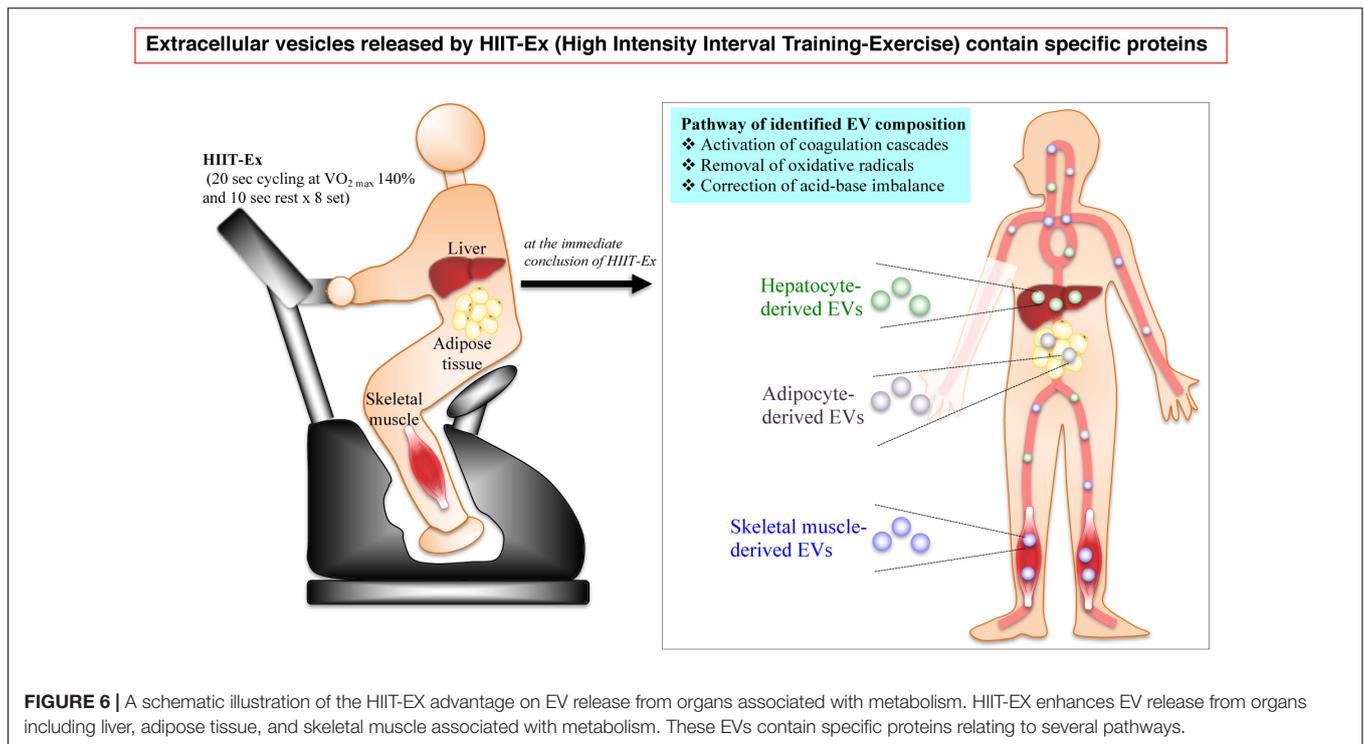
FIGURE 5 | Proteomics analysis of EV proteins. **(A)** Proteomics analysis was performed on the EV proteins changed among at pre-HIIT-Ex, T_0, and T_{30}. **(B)** Representative immunoblotting of CAT and PRDX-2 in circulating EVs before (pre) and at T_0. **(C)** Abundance ratio of EV protein expression, CAT and PRDX-2, in circulating EVs at T_0 compared to pre-HIIT-EX, which was quantified using Multi Gauge software. Pre: pre-HIIT-Ex.

into oxygen and water (H_2O). Our results were consistent with the previous report in which it was demonstrated that plasma CAT levels were significantly increased at 3 and 24 h after HIIT-Ex (Bessa et al., 2016). PRDX-2, a member of the PRDX family, is abundant in erythrocytes, skeletal muscle, and cardiac muscle (Brinkmann and Brixius, 2013). Moghaddam et al. (2011) reported that PRDX-2 in erythrocytes was upregulated *via* physical training (3 months, three times a week, cycling for 25–50 min at 75% of maximal heart rate) in patients with type 2 diabetes. Conversely, another study reported that there was no

FIGURE 6 | A schematic illustration of the HIIT-EX advantage on EV release from organs associated with metabolism. HIIT-EX enhances EV release from organs including liver, adipose tissue, and skeletal muscle associated with metabolism. These EVs contain specific proteins relating to several pathways.

change in skeletal muscle PRDX-2 expression in patients with type 2 diabetes after training (3 months, twice a week, cycling for 25–50 min at heart rate corresponding to 2 n mon/L blood lactate concentration) (Brinkmann et al., 2012). The current study revealed that these antioxidant enzymes were encapsulated in EVs of circulating blood, although we need to investigate the regulation manner of the encapsulated PRDX-2 driven by HIIT-Ex in future studies.

CA and PRDX-2 have been identified as significant elevated EV-packed proteins in different types of Ex, such as 2-km run (Wu and Liu, 2018) and 1 h bout of cycling Ex (Whitham et al., 2018). We demonstrated these proteins encapsulated in EVs were promptly released into circulation in response to only 4 min of HIIT-Ex, suggesting they can be used as biomarkers for HIIT-Ex with a particularly short time, as well as other type of Ex, although we needed further validation in larger cohorts.

The present study has some limitations. (1) The current study was a prospective single-arm study, not a randomized study with a control group. (2) The sample number of proteomics analysis was limited due to expensive cost. In the current study, proteomics analysis at pre-HIIT-Ex, T_0, and T_{30} was performed on three subjects. We detected catalase and PRX2 in the remaining 14 subjects by Western blotting. In the future, we need to validate the current results with proteomics analysis in a larger number of samples.

CONCLUSION

In conclusion, the circulating EV numbers and protein composition can be immediately changed after 0 and/or 30 min by a particularly short time of HIIT-Ex. A part of circulating EVs were derived from multiple tissues and cells including the skeletal muscle, hepatocytes, and adipose tissue as a function of HIIT-Ex. Furthermore, the protein composition of EVs involved in activating coagulation cascades, removal of oxidative stress, and correction of acid–base imbalance was identified by proteomic analysis. These results indicated that EVs intercommunicate across various organs rapidly in response to HIIT-Ex (**Figure 6**).

DATA AVAILABILITY STATEMENT

The datasets presented in this study can be found in online repositories. The names of the repository/repositories and accession number(s) can be found below: https://doi.org/10.6084/m9.figshare.13480317.v1.

ETHICS STATEMENT

The studies involving human participants were reviewed and approved by the Ethics Committee at Mie University. The patients/participants provided their written informed consent to participate in this study.

AUTHOR CONTRIBUTIONS

AE, YK, and KT contributed to conception and design of the study. YK, AE, MI, and YTak organized the database.

YTam, MT, and KI performed the experiments. SF performed the statistical analysis. YK wrote the first draft of the manuscript. AE and SF wrote sections of the manuscript. All authors contributed to manuscript revision, read, and approved the submitted version.

SUPPLEMENTARY MATERIAL

The Supplementary Material for this article can be found online at: https://www.frontiersin.org/articles/10.3389/fphys.2021.693007/full#supplementary-material

Supplementary Figure 1 | The whole membrane of Western blotting for **Figure 3B**.

Supplementary Figure 2 | The whole membrane of Western blotting for **Figure 5E**.

Supplementary Table 1 | Biochemical parameters before and after HIIT-Ex.

Supplementary Table 2 | The list of proteins.

REFERENCES

Ashwell, G., and Morell, A. G. (1974). The role of surface carbohydrates in the hepatic recognition and transport of circulating glycoproteins. *Adv. Enzymol. Relat. Areas Mol. Biol.* 41, 99–128. doi: 10.1002/9780470122860.ch3

Babicki, S., Arndt, D., Marcu, A., Liang, Y., Grant, J. R., Maciejewski, A., et al. (2016). Heatmapper: web-enabled heat mapping for all. *Nucleic Acids Res.* 44, W147–W153.

Bessa, A. L., Oliveira, V. N., Agostini, G. G., Oliveira, R. J., Oliveira, A. C., White, G. E., et al. (2016). Exercise Intensity and Recovery: biomarkers of Injury, Inflammation, and Oxidative Stress. *J. Strength Cond. Res.* 30, 311–319. doi: 10.1519/jsc.0b013e31828f1ee9

Brinkmann, C., and Brixius, K. (2013). Peroxiredoxins and sports: new insights on the antioxidative defense. *J. Physiol. Sci.* 63, 1–5. doi: 10.1007/s12576-012-0237-4

Brinkmann, C., Chung, N., Schmidt, U., Kreutz, T., Lenzen, E., Schiffer, T., et al. (2012). Training alters the skeletal muscle antioxidative capacity in non-insulin-dependent type 2 diabetic men. *Scand. J. Med. Sci. Sports* 22, 462–470. doi: 10.1111/j.1600-0838.2010.01273.x

Buchheit, M., and Laursen, P. B. (2013a). High-intensity interval training, solutions to the programming puzzle. Part I: cardiopulmonary emphasis. *Sports Med.* 43, 313–338. doi: 10.1007/s40279-013-0029-x

Buchheit, M., and Laursen, P. B. (2013b). High-intensity interval training, solutions to the programming puzzle. Part II: anaerobic energy, neuromuscular load and practical applications. *Sports Med.* 43, 927–954. doi: 10.1007/s40279-013-0066-5

Davis, R. A. H., Halbrooks, J. E., Watkins, E. E., Fisher, G., Hunter, G. R., Nagy, T. R., et al. (2017). High-intensity interval training and calorie restriction promote remodeling of glucose and lipid metabolism in diet-induced obesity. *Am. J. Physiol. Endocrinol. Metab.* 313, E243–E256.

Denham, J., and Spencer, S. J. (2020). Emerging roles of extracellular vesicles in the intercellular communication for exercise-induced adaptations. *Am. J. Physiol. Endocrinol. Metab.* 319, E320–E329.

Dillard, C. J., Litov, R. E., Savin, W. M., Dumelin, E. E., and Tappel, A. L. (1978). Effects of exercise, vitamin E, and ozone on pulmonary function and lipid peroxidation. *J. Appl. Physiol. Respir. Environ. Exerc. Physiol.* 45, 927–932. doi: 10.1152/jappl.1978.45.6.927

Eguchi, A., Lazic, M., Armando, A. M., Phillips, S. A., Katebian, R., Maraka, S., et al. (2016). Circulating adipocyte-derived extracellular vesicles are novel markers of metabolic stress. *J. Mol. Med.* 94, 1241–1253. doi: 10.1007/s00109-016-1446-8

Forterre, A., Jalabert, A., Berger, E., Baudet, M., Chikh, K., Errazuriz, E., et al. (2014). Proteomic analysis of C2C12 myoblast and myotube exosome-like vesicles: a new paradigm for myoblast-myotube cross talk? *PLoS One* 9:e84153. doi: 10.1371/journal.pone.0084153

Fruhbeis, C., Helmig, S., Tug, S., Simon, P., and Kramer-Albers, E. M. (2015). Physical exercise induces rapid release of small extracellular vesicles into the circulation. *J. Extracell. Vesicles* 4:28239. doi: 10.3402/jev.v4.28239

Gray, W. D., Mitchell, A. J., and Searles, C. D. (2015). An accurate, precise method for general labeling of extracellular vesicles. *MethodsX* 2, 360–367. doi: 10.1016/j.mex.2015.08.002

Guescini, M., Guidolin, D., Vallorani, L., Casadei, L., Gioacchini, A. M., Tibollo, P., et al. (2010). C2C12 myoblasts release micro-vesicles containing mtDNA and proteins involved in signal transduction. *Exp. Cell Res.* 316, 1977–1984. doi: 10.1016/j.yexcr.2010.04.006

Highton, P. J., Goltz, F. R., Martin, N., Stensel, D. J., Thackray, A. E., and Bishop, N. C. (2019). Microparticle Responses to Aerobic Exercise and Meal Consumption in Healthy Men. *Med. Sci. Sports Exerc.* 51, 1935–1943. doi: 10.1249/mss.0000000000001985

Ilkovski, B., Clement, S., Sewry, C., North, K. N., and Cooper, S. T. (2005). Defining alpha-skeletal and alpha-cardiac actin expression in human heart and skeletal muscle explains the absence of cardiac involvement in ACTA1 nemaline myopathy. *Neuromuscul. Disord.* 15, 829–835. doi: 10.1016/j.nmd.2005.08.004

Kalluri, R., and LeBleu, V. S. (2020). The biology, function, and biomedical applications of exosomes. *Science* 367:eaau6977. doi: 10.1126/science.aau6977

Kimmel, A. R., Brasaemle, D. L., Mcandrews-Hill, M., Sztalryd, C., and Londos, C. (2010). Adoption of PERILIPIN as a unifying nomenclature for the mammalian PAT-family of intracellular lipid storage droplet proteins. *J. Lipid Res.* 51, 468–471. doi: 10.1194/jlr.r000034

Kobayashi, Y., Eguchi, A., Tempaku, M., Honda, T., Togashi, K., Iwasa, M., et al. (2018). Circulating extracellular vesicles are associated with lipid and insulin metabolism. *Am. J. Physiol. Endocrinol. Metab.* 315, E574–E582.

Laursen, P. B., and Jenkins, D. G. (2002). The scientific basis for high-intensity interval training: optimising training programmes and maximising performance in highly trained endurance athletes. *Sports Med.* 32, 53–73. doi: 10.2165/00007256-200232010-00003

Matthews, D. R., Hosker, J. P., Rudenski, A. S., Naylor, B. A., Treacher, D. F., and Turner, R. C. (1985). Homeostasis model assessment: insulin resistance and beta-cell function from fasting plasma glucose and insulin concentrations in man. *Diabetologia* 28, 412–419. doi: 10.1007/bf00280883

Moghaddam, D. A., Heber, A., Capin, D., Kreutz, T., Opitz, D., Lenzen, E., et al. (2011). Training increases peroxiredoxin 2 contents in the erythrocytes of overweight/obese men suffering from type 2 diabetes. *Wien. Med. Wochenschr.* 161, 511–518. doi: 10.1007/s10354-011-0037-0

Nederveen, J. P., Warnier, G., Di Carlo, A., Nilsson, M. I., and Tarnopolsky, M. A. (2020). Extracellular Vesicles and Exosomes: insights From Exercise Science. *Front. Physiol.* 11:604274. doi: 10.3389/fphys.2020.604274

No authors listed. (2000). Obesity: preventing and managing the global epidemic. Report of a WHO consultation. *World Health Organ. Tech. Rep. Ser.* 894, 1–253.

Povero, D., Eguchi, A., Li, H., Johnson, C. D., Papouchado, B. G., Wree, A., et al. (2014). Circulating extracellular vesicles with specific proteome and liver microRNAs are potential biomarkers for liver injury in experimental fatty liver disease. *PLoS One* 9:e113651. doi: 10.1371/journal.pone.0113651

Powers, S. K., and Jackson, M. J. (2008). Exercise-induced oxidative stress: cellular mechanisms and impact on muscle force production. *Physiol. Rev.* 88, 1243–1276. doi: 10.1152/physrev.00031.2007

Powers, S. K., Radak, Z., and Ji, L. L. (2016). Exercise-induced oxidative stress: past, present and future. *J. Physiol.* 594, 5081–5092. doi: 10.1113/jp270646

Reid, M. B., Shoji, T., Moody, M. R., and Entman, M. L. (1992). Reactive oxygen in skeletal muscle. II. Extracellular release of free radicals. *J. Appl. Physiol.* 73, 1805–1809. doi: 10.1152/jappl.1992.73.5.1805

Rome, S., Forterre, A., Mizgier, M. L., and Bouzakri, K. (2019). Skeletal Muscle-Released Extracellular Vesicles: state of the Art. *Front. Physiol.* 10:929. doi: 10.3389/fphys.2019.00929

Sogaard, D., Lund, M. T., Scheuer, C. M., Dehlbaek, M. S., Dideriksen, S. G., Abildskov, C. V., et al. (2018). High-intensity interval training improves insulin sensitivity in older individuals. *Acta Physiol.* 222:e13009. doi: 10.1111/apha.13009

Szklarczyk, D., Gable, A. L., Lyon, D., Junge, A., Wyder, S., Huerta-Cepas, J., et al. (2019). STRING v11: protein-protein association networks with increased coverage, supporting functional discovery in genome-wide experimental datasets. *Nucleic Acids Res.* 47, D607–D613.

Tabata, I., Nishimura, K., Kouzaki, M., Hirai, Y., Ogita, F., Miyachi, M., et al. (1996). Effects of moderate-intensity endurance and high-intensity intermittent training on anaerobic capacity and VO2max. *Med. Sci. Sports Exerc.* 28, 1327–1330. doi: 10.1097/00005768-199610000-00018

Tas, M., Senturk, E., Ekinci, D., Demirdag, R., Comakli, V., Bayram, M., et al. (2019). Comparison of blood carbonic anhydrase activity of athletes performing interval and continuous running exercise at high altitude.

J. Enzyme Inhib. Med. Chem. 34, 218–224. doi: 10.1080/14756366.2018.1545768

Tkach, M., and Thery, C. (2016). Communication by Extracellular Vesicles: where We Are and Where We Need to Go. *Cell* 164, 1226–1232. doi: 10.1016/j.cell.2016.01.043

Vechetti, I. J. Jr. (2019). Emerging role of extracellular vesicles in the regulation of skeletal muscle adaptation. *J. Appl. Physiol.* 127, 645–653. doi: 10.1152/japplphysiol.00914.2018

Vechetti, I. J. Jr., Valentino, T., Mobley, C. B., and Mccarthy, J. J. (2020). The role of extracellular vesicles in skeletal muscle and systematic adaptation to exercise. *J. Physiol.* 599, 845–861. doi: 10.1113/jp278929

Whitham, M., Parker, B. L., Friedrichsen, M., Hingst, J. R., Hjorth, M., Hughes, W. E., et al. (2018). Extracellular Vesicles Provide a Means for Tissue Crosstalk during Exercise. *Cell Metab.* 27, 237–251.e4.

Wu, C. X., and Liu, Z. F. (2018). Proteomic Profiling of Sweat Exosome Suggests its Involvement in Skin Immunity. *J. Invest. Dermatol.* 138, 89–97.

Zadow, E. K., Kitic, C. M., Wu, S. S. X., Fell, J. W., and Adams, M. J. (2018). Time of day and short-duration high-intensity exercise influences on coagulation and fibrinolysis. *Eur. J. Sport Sci.* 18, 367–375.